 CMC, vol.34, no.2, pp.143-175, 2013

# A New Optimal Iterative Algorithm for Solving Nonlinear Poisson Problems in Heat Diffusion

**Chih-Wen Chang**[1,2], **Chein-Shan Liu**[3]

**Abstract:** The nonlinear Poisson problems in heat diffusion governed by elliptic type partial differential equations are solved by a modified globally optimal iterative algorithm (MGOIA). The MGOIA is a purely iterative method for searching the solution vector **x** without using the invert of the Jacobian matrix **D**. Moreover, we reveal the weighting parameter $\alpha_c$ in the best descent vector $\mathbf{w} = \alpha_c \mathbf{E} + \mathbf{D}^{\mathrm{T}}\mathbf{E}$ and derive the convergence rate and find a criterion of the parameter $\gamma$. When utilizing $\alpha_c$ and $\gamma$, we can further accelerate the convergence speed several times. Several numerical experiments are carefully discussed and validated the proposed method.

**Keywords:** Nonlinear algebraic equations, Nonlinear Poisson equation, Iterative algorithm, Modified globally optimal iterative algorithm (MGOIA) Invariant manifold

## 1 Introduction

Poisson problems that arise from engineering applications are often classified as linear Poisson problems and nonlinear Poisson problems. In most cases, solving those nonlinear problems analytically and exactly is impossible, or at least highly impractical. Therefore, numerical approaches such as the Lagrangian finite difference method (FDM) and finite element method (FEM) are often utilized to calculate the linear Poisson problems [Whiteman (1974)]; however, these two methods cost much computer time. Then, because the mesh construction of domain is time-consuming and cannot always be totally automated, Gu (1991) used the boundary element method (BEM) to solve the linear Poisson problems. Nevertheless, the mesh generation of boundary still increases the computation time and computer storage necessity. Comparing with those mesh-dependent algorithms such as

[1] Cloud Computing and System Integration Division, National Center for High-Performance Computing, Taichung 40763, Taiwan.
[2] Corresponding author, Tel.:+886-4-24620202#860. E-mail address: 0903040@nchc.narl.org.tw
[3] Department of Civil Engineering, National Taiwan University, Taipei 10617, Taiwan.

the FDM, FEM and BEM, the method of fundamental solutions [Golberg (1995)], which does not require any boundary or domain discretization, has been proposed.

For the nonlinear Poisson problems, Kasab, Karur and Ramachandran (1995) analyzed the quasilinear BEM for solving two-dimensional nonlinear Poisson type problems. They claimed that their method provides extremely accurate results for mildly nonlinear forcing functions. For strongly nonlinear forcing functions, the approach is employed at a subdomain level and produces good results with only a few subdomains; however, their scheme is complex and hard to implement. Recently, several meshless schemes have been proposed to resolve the nonlinear Poisson problems, like that demonstrated by Balakrishnan and Ramachandran (1999), Zhu, Zhang and Atluri (1999), Balakrishnan and Ramachandran (2001), Tri, Zahrouni and Potier-Ferry (2011), Tri, Zahrouni and Potier-Ferry (2012), and Wang, Qin and Liang (2012), which did not need to deal with the discretization of the entire domain and boundary. After that, Liu (2008, 2009) proposed the fictitious time integration method (FTIM) to tackle the elliptic boundary value problems, of which the FTIM was local convergence and needed to choose the viscous damping coefficients for different equations in one problem. Later, Liu and his coworkers [Liu, Dai and Atluri (2011a); Liu, Dai and Atluri (2011b); Liu (2012); Liu and Atluri (2012)] employed the technique of optimal iterative algorithms to solve a large system of nonlinear algebraic equations, and demonstrated that high performance can be achieved by using these approaches. Furthermore, we modify the globally optimal iterative algorithm in Liu and Atluri (2012) and obtain a faster convergence optimal iterative algorithm in this study.

This research is organized as follows. Section 2 demonstrates a theoretical basis of the proposed scheme. We begin from a continuous manifold defined in terms of residual-norm, and arrive at a system of ordinary differential equations (ODEs) driven by a vector, which is a combination of the vectors $\mathbf{E}$ and $\mathbf{D}^{\mathrm{T}}\mathbf{E}$, where $\mathbf{D}$ is the Jacobian. Section 3 is dedicated to deriving a scalar equation to keep the discretely iterative orbit on the manifold, and then we propose two new concepts of optimal descent vector and best descent vector to choose the optimal and critical parameters $\alpha_0$ and $\alpha_c$, which automatically have a convergent behavior of the residual-error curve, and derive a switch criterion of $\gamma$. In Section 4, we employ the present approach with different convergent rates to resolve four numerical experiments of nonlinear Poisson problems. At last, some concluding remarks are drawn in Section 5.

## 2 An invariant manifold

In this study, we propose a new iterative approach to solve a system of nonlinear algebraic equations (NAEs): $E_i(x_1,\ldots,x_n) = 0$, $i$ =1,…, $n$, or in their vector-form:

$$\mathbf{E}(\mathbf{x}) = \mathbf{0}. \tag{1}$$

For the NAEs in Eq. (1), we can formulate a scalar Newton homotopy function:

$$g(\mathbf{x},\, t) = \frac{Q(t)\,\|\mathbf{E}(\mathbf{x})\|^2}{2} - \frac{\|\mathbf{E}(\mathbf{x}_0)\|^2}{2} = 0, \tag{2}$$

in which, we let $\mathbf{x}$ be a function of a fictitious time-like variable $t$, and its initial value is $\mathbf{x}(0) = \mathbf{x}_0$.

We anticipate $g(\mathbf{x},\, t) = 0$ to be an invariant manifold in the space of $(\mathbf{x},\, t)$ for a dynamical system $g(\mathbf{x}(t),\, t) = 0$ to be specified further. While $Q > 0$, the manifold clarified by Eq. (2) is continuous, and therefore the following operation of differential accomplished on the manifold makes sense [Liu and Atluri (2011a)]. As a "consistency condition", by taking the time differential of Eq. (2) with respect to $t$ and contemplating $\mathbf{x} = \mathbf{x}(t)$, we obtain

$$\frac{\dot{Q}(t)\,\|\mathbf{E}(\mathbf{x})\|^2}{2} - Q(t)(\mathbf{D}^{\mathrm{T}}\mathbf{E})\cdot\dot{\mathbf{x}} = 0. \tag{3}$$

We presume that the evolution of $\mathbf{x}$ is driven by a vector $\mathbf{w}$:

$$\dot{\mathbf{x}} = \lambda\mathbf{w}, \tag{4}$$

where $\lambda$ in general is a scalar function of $t$, and

$$\mathbf{w} = \alpha\mathbf{E} + \mathbf{D}^{\mathrm{T}}\mathbf{E}, \tag{5}$$

is a suitable combination of the residual vector $\mathbf{E}$ as well as the gradient vector $\mathbf{D}^{\mathrm{T}}\mathbf{E}$, and is $\alpha$ a parameter to be optimized below. Inserting Eq. (4) into Eq. (3), we can derive

$$\dot{\mathbf{x}} = -p(t)\frac{\|\mathbf{E}\|^2}{\mathbf{E}^{\mathrm{T}}\mathbf{q}}\mathbf{w}, \tag{6}$$

in which

$$\mathbf{F} := \mathbf{D}\mathbf{D}^{\mathrm{T}} \tag{7}$$

$$\mathbf{q} := \mathbf{D}\mathbf{w} = \mathbf{q}_1 + \alpha\mathbf{q}_2 = \mathbf{F}\mathbf{E} + \alpha\mathbf{D}\mathbf{E} \tag{8}$$

$$p(t) := \frac{\dot{Q}(t)}{2Q(t)}. \tag{9}$$

Thus, in this scheme if $Q(t)$ can be promised to be a monotonically increasing function of $t$, we may have an absolutely convergent property in solving the NAEs in Eq. (1):

$$\|\mathbf{E}(\mathbf{x})\|^2 = \frac{C}{Q(t)}, \tag{10}$$

where

$$C = \|\mathbf{E}(\mathbf{x}_0)\|^2 \tag{11}$$

is chosen by the initial value $\mathbf{x}_0$. We do not require to specify the function $Q(t)$ a priori; however, $\sqrt{C/Q(t)}$ only acts as a measure of the residual error of $\mathbf{E}$ at the same time. Hence, we impose on our scheme that $Q(t) > 0$ is a monotonically increasing function of $t$. When $t$ is enormous, the above equation will compel the residual error $\|\mathbf{E}(\mathbf{x})\|$ to tend to zero, and meanwhile the solution of Eq. (1) is acquired accessibly.

## 3 Dynamics of the proposed iterative scheme

### *3.1 Discretizing, yet keeping x on the manifold*

We discretize the foregoing continuous time dynamics embodied in Eq. (6) into a discrete time dynamics:

$$\mathbf{x}(t+\Delta t) = \mathbf{x}(t) - \beta \frac{\|\mathbf{E}\|^2}{\mathbf{E}^{\mathrm{T}}\mathbf{q}}\mathbf{w}, \tag{12}$$

where

$$\beta = p(t)\Delta t \tag{13}$$

is the step-length. Eq. (10) is acquired from the ODEs in Eq. (6) by employing the Euler algorithm.

To keep $\mathbf{x}$ on the manifold defined by Eq. (10), we can ponder the evolution of $\mathbf{E}$ along the path $\mathbf{x}(t)$ by

$$\dot{\mathbf{E}} = \mathbf{D}\dot{\mathbf{x}} = -p(t)\frac{\|\mathbf{E}\|^2}{\mathbf{E}^{\mathrm{T}}\mathbf{q}}\mathbf{q}. \tag{14}$$

Similarly, we utilize the Euler algorithm to integrate Eq. (14) and acquire

$$\mathbf{E}(t+\Delta t) = \mathbf{E}(t) - \beta \frac{\|\mathbf{E}\|^2}{\mathbf{E}^{\mathrm{T}}\mathbf{q}}\mathbf{q}, \tag{15}$$

Taking the square-norms of both the sides of Eq. (15) and employing Eq. (10), we can acquire

$$\frac{C}{Q(t+\Delta t)} = \frac{C}{Q(t)} - 2\beta\frac{C}{Q(t)} + \beta^2\frac{C}{Q(t)}\frac{\|\mathbf{E}\|^2}{(\mathbf{E}^{\mathrm{T}}\mathbf{q})^2}\|\mathbf{q}\|^2. \tag{16}$$

Hence, by dividing both the sides by $C/Q(t)$, we can derive the following scalar equation:

$$a_0\beta^2 - 2\beta + 1 - \frac{Q(t)}{Q(t+\Delta t)} = 0, \tag{17}$$

in which

$$a_0 := \frac{\|\mathbf{E}\|^2\|\mathbf{q}\|^2}{(\mathbf{E}^{\mathrm{T}}\mathbf{q})^2} \geq 1, \tag{18}$$

by employing the Cauchy-Schwarz inequality.

Consequently, $g(\mathbf{x}, t) = 0$, $t \in \{0, 1, 2, \ldots\}$ remains to be an invariant manifold in the space of $(\mathbf{x}, t)$ for the discrete time dynamical system $g(\mathbf{x}(t), t) = 0$, which will be explored further in the next two sections. Liu and Atluri (2011a) first derived the formulae (15) and (16) for a simply gradient-vector driven dynamical system.

### *3.2 A discrete dynamics*

Let

$$s = \frac{Q(t)}{Q(t+\Delta t)} = \frac{\|\mathbf{E}(\mathbf{x}(t+\Delta t))\|^2}{\|\mathbf{E}(\mathbf{x}(t))\|^2}, \tag{19}$$

which is a significant quantity to evaluate the convergence property of numerical scheme for solving NAEs. If $s$ can be promised to be $s < 1$, then the residual error $\|\mathbf{E}\|$ will be decreased step-by-step in the iteration process.

From Eqs. (17) and (19), we can acquire

$$a_0\beta^2 - 2\beta + 1 - s = 0, \tag{20}$$

of which we can take the solution of $\beta$ to be

$$\beta = \frac{1 - \sqrt{1-(1-s)a_0}}{a_0}, \text{ if } 1-(1-s)a_0 \geq 0. \tag{21}$$

Let

$$1-(1-s)a_0=\gamma^2\geq 0, \tag{22}$$

$$s=1-\frac{1-\gamma^2}{a_0}; \tag{23}$$

and the condition $1-(1-s)a_0\geq 0$ in Eq. (21) is automatically satisfied. Hence, we can obtain

$$\beta=\frac{1-\gamma}{a_0}, \tag{24}$$

and from Eqs. (12), (18) and (24), we can acquire the approach as follows:

$$\mathbf{x}(t+\Delta t)=\mathbf{x}(t)-(1-\gamma)\frac{\mathbf{E}^{\mathrm{T}}\mathbf{q}}{\|\mathbf{q}\|^2}\mathbf{w}, \tag{25}$$

in which $0\leq\gamma<1$ is a weighting parameter. Under the above condition, we can prove that the new scheme satisfies

$$\text{Convergence Rate} := \frac{\|\mathbf{E}(t)\|}{\|\mathbf{E}(t+\Delta t)\|}=\frac{1}{\sqrt{s}}>1. \tag{26}$$

We do not need $\Delta t$ to be integrated in the above method. Moreover, the property is significant because it promises the new approach to be absolutely convergent to the true solution.

### *3.3 An alternate value of relaxation parameter*

In the above section, the relaxation parameter $\gamma$ is not specified yet. We will derive a formula about $\gamma$.

By utilizing the Euler approach, we have

$$\dot{Q}(t)\Delta t=Q(t+\Delta t)-Q(t). \tag{27}$$

From Eqs. (9), (13), (19) and (27), we obtain

$$\beta=p(t)\Delta t=\frac{\dot{Q}(t)\Delta t}{2Q(t)}=\frac{1}{2s}-\frac{1}{2}. \tag{28}$$

Then by using Eqs. (24) and (28), we can acquire

$$s=\frac{1}{2\beta+1}=\frac{a_0}{a_0+2-2r}. \tag{29}$$

On the other hand, Eq. (23) renders

$$s = \frac{a_0 - 1 + r^2}{a_0}. \tag{30}$$

By equating the two $s$ in the above two equations, we can derive a third-order scalar equation for $r$:

$$2r^3 - (a_0+2)r^2 + 2(a_0-1)r - a_0 + 2 = 0. \tag{31}$$

Furthermore, we can decompose the above equation into

$$2(r-1)^2(r - \frac{a_0}{2} + 1) = 0, \tag{32}$$

in which $r = 1$ is the double roots, which is not the desired one in view of $0 \le r < 1$, and another is

$$r = \frac{a_0}{2} - 1, \text{ if } 2 \le a_0 < 4, \tag{33}$$

where, we impose the condition of $2 \le a_0 < 4$ to satisfy $0 \le r < 1$.
From Eqs. (9), (13) and (27), it follows that

$$\beta = \frac{1}{2}(R-1), \tag{34}$$

where the ratio $R$ is defined by

$$R := \frac{Q(t+\Delta t)}{Q(t)} = \frac{1}{s}. \tag{35}$$

Inserting Eqs. (34) and (35) into Eq.(20), we can derive

$$a_0 R^3 - 2(a_0+2)R^2 + (a_0+8)R - 4 = 0. \tag{36}$$

Note that the above equation can be written as

$$(R-1)^2(a_0 R - 4) = 0. \tag{37}$$

To satisfy the requirement of $\dot{Q}(t) > 0$, we require $R > 1$. Because $R = 1$ is the double roots and it is not the desired one, we can take

$$R = \frac{4}{a_0}. \tag{38}$$

Hence, besides Eqs. (29) and (30), by Eqs. (35) and (38) we have acquired the third representation of $s$:

$$s = \frac{a_0}{4}. \tag{39}$$

By equating Eqs. (36) and (26), we obtain the same solution for $r$ as that in Eq. (30). Nevertheless, if we let the two $s$ in Eqs. (36) and (27) be equal, we can solve

$$r^2 = (\frac{a_0}{2} - 1)^2. \tag{40}$$

In summary, we can set

$$r = \left| \frac{a_0}{2} - 1 \right|, \text{ if } a_0 < 4, \tag{41}$$

where we restrict $a_0 < 4$ to satisfy $0 \leq r < 1$.

### *3.4 The method driven by the optimal descent vector w = $\alpha_0$E+$D^T$E*

The scheme (25) does not specify how to determine the parameter $\alpha$. We can choose a suitable $\alpha$ such that $s$ clarified in Eq. (23) is minimized with respect to $\alpha$, because a smaller $s$ will result in a faster convergence as displayed in Eq. (26).

Therefore, by inserting Eq. (18) for $a_0$ into Eq. (31), we can obtain $s$ as follows:

$$s = 1 - \frac{(1-\gamma^2)(\mathbf{E}\cdot\mathbf{q})^2}{\|\mathbf{E}\|^2 \|\mathbf{q}\|^2}, \tag{42}$$

where $\mathbf{q}$ as defined by Eq. (8) includes a parameter $\alpha$. Let $\partial s/\partial\alpha = 0$, and through some algebraic operations we can resolve $\alpha$ by

$$\alpha_0 = \frac{[\mathbf{q}_1, \mathbf{E}, \mathbf{q}_2]\cdot\mathbf{q}_1}{[\mathbf{q}_2, \mathbf{E}, \mathbf{q}_1]\cdot\mathbf{q}_2}. \tag{43}$$

where

$$[\mathbf{a}, \mathbf{b}, \mathbf{c}] = (\mathbf{a}\cdot\mathbf{b})\mathbf{c} - (\mathbf{c}\cdot\mathbf{b})\mathbf{a}, \quad \mathbf{a},\mathbf{b},\mathbf{c} \in \mathbb{R}^n \tag{44}$$

is defined by Liu (2000) for a Jordan algebra. Inserting the above $\alpha_0$ into Eq. (5), we can acquire the optimal vector:

$$\mathbf{w} = \alpha_0\mathbf{E} + \mathbf{D}^{\mathrm{T}}\mathbf{E}\,. \tag{45}$$

### 3.5 A critical value for $\alpha$

Previously, Liu and Atluri (2011b) have derived the optimal $\alpha$ in the descent vector $\mathbf{w} = \alpha\mathbf{E}+(1-\alpha)\mathbf{D}^{\mathrm{T}}\mathbf{E}$ by letting $\partial s/\partial\alpha = 0$. In Section 3.4, we have utilized $\partial s/\partial\alpha = 0$ (or equivalently, $\partial a_0/\partial\alpha = 0$) to reveal the optimal value of $\alpha$ in the descent vector $\mathbf{w} = \alpha\mathbf{E}+\mathbf{D}^{\mathrm{T}}\mathbf{E}$. Usually, this value of $\alpha$ acquired from $\partial s/\partial\alpha = 0$ is not the global minimum of $a_0$ (or $s$), and instead of a local minimum. We try another scheme and attempt to develop a more powerful choice principle of $\alpha$, such that the value of $\alpha$ acquired is the global minimum of $a_0$ (or $s$); however, before that we give a remark about the best selection of the descent vector $\mathbf{w}$.

**Remark 1:** The best choice of $\mathbf{w}$ would be $\mathbf{w} = \mathbf{D}^{-1}\mathbf{E}$, which by Eq. (8) results in $\mathbf{q} = \mathbf{E}$, and by Eq. (18) further results in the smallest value of $a_0 = 1$. If $\mathbf{w} = \mathbf{D}^{-1}\mathbf{E}$ is realizable, we obtain $s = \gamma^2$ by Eq. (23), and therefore from Eq. (26), we have an infinite convergence rate by letting $\gamma = 0$, which can reveal the solution with one step. In this regard, $\mathbf{D}^{-1}\mathbf{E}$ is the best vector and is the best descent direction for a numerical scheme used to resolve Eq. (1). The Newton iterative method is of this type; nevertheless, it is very hard to be realized in a numerical algorithm because $\mathbf{D}^{-1}$ is difficult to reveal.

In accordance with the following equivalent relation:

$$a_0 = 1 \equiv \mathbf{w} = \mathbf{D}^{-1}\mathbf{E} \tag{46}$$

we introduce a new approach to estimate the best vector in our framework of optimal iterative scheme.

Motivated by the above remark about the best vector, which is very hard to obtain in practice, we can slightly relax the necessary of the value of $a_0$ to be 1. It means that we can relax the choice of $\mathbf{w} = \mathbf{D}^{-1}\mathbf{E}$ by Eq. (46). Instead of, we can decide a suitable $\alpha$ such that $a_0$ defined by Eq. (18) takes a suitable small value $a_s > 1$. That is

$$a_0 := \frac{\|\mathbf{E}\|^2 \|\mathbf{q}\|^2}{(\mathbf{E}^{\mathrm{T}}\mathbf{q})^2} = a_s. \tag{47}$$

When $a_s$ is near to 1, the convergence speed is very fast. Inserting Eq. (8) for $\mathbf{q}$ into the above equation, and through some elementary operations we can derive a quadratic equation to solve $\alpha$:

$$e_1\alpha^2 + e_2\alpha + e_3 = 0, \tag{48}$$

where

$$e_1 := \|\mathbf{E}\|^2 \|\mathbf{q}_2\|^2 - a_s(\mathbf{E}\cdot\mathbf{q}_2)^2, \tag{49}$$

$$e_2 := 2\|\mathbf{E}\|^2 \mathbf{q}_2 \cdot \mathbf{q}_1 - 2a_s \mathbf{E}\cdot\mathbf{q}_1 \mathbf{E}\cdot\mathbf{q}_2, \tag{50}$$

$$e_3 := \|\mathbf{E}\|^2 \|\mathbf{q}_1\|^2 - a_s(\mathbf{E}\cdot\mathbf{q}_1)^2. \tag{51}$$

If the following condition is satisfied

$$D := e_2^2 - 4e_1e_3 \geq 0, \tag{52}$$

then $\alpha$ has a real solution:

$$\alpha = \frac{\sqrt{D} - e_2}{2e_1}. \tag{53}$$

Inserting Eqs. (49)-(51) into the critical equation:

$$D := e_2^2 - 4e_1e_3 = 0, \tag{54}$$

we can derive an algebraic equation to decide which $a_s$ is the lowest bound of Eq. (52) of which the equality holds. In this lowest bound $a_s$ is a critical value denoted by $a_c$, and for all $a_s \geq a_c$ it can satisfy Eq. (52). From Eq. (54) through some operations, the critical value $a_c$ can be solved as:

$$a_c := \frac{\|\mathbf{E}\|^2 [\|\mathbf{q}_1\|^2 \|\mathbf{q}_2\|^2 - (\mathbf{q}_1\cdot\mathbf{q}_2)^2]}{\|[\mathbf{q}_1, \mathbf{E}, \mathbf{q}_2]\|^2}. \tag{55}$$

Then, inserting it for $a_s$ into Eqs. (49) and (50), we can acquire a critical value $\alpha_c$ for $\alpha$ from Eq. (53)

$$\alpha_c := \frac{a_c \mathbf{E}\cdot\mathbf{q}_1 \mathbf{E}\cdot\mathbf{q}_2 - \|\mathbf{E}\|^2 \mathbf{q}_1\cdot\mathbf{q}_2}{\|\mathbf{E}\|^2 \|\mathbf{q}_2\|^2 - a_c(\mathbf{E}\cdot\mathbf{q}_2)^2}, \tag{56}$$

such that

$$\mathbf{w} = \alpha_c \mathbf{E} + \mathbf{D}^{\mathrm{T}}\mathbf{E} \quad \text{(best descent vector)} \tag{57}$$

is the best descent vector, which is in practice the best approximation to the real best vector $\mathbf{w} = \mathbf{D}^{-1}\mathbf{E}$ employed in the Newton iterative scheme. Owing to its critically, if one attempts to reveal a better value than $\alpha_c$, there would be no real solution of $\alpha$. Moreover, the current best descent vector is also better than the optimal descent vector $\mathbf{w} = \alpha_0\mathbf{E}+\mathbf{D}^{\mathrm{T}}\mathbf{E}$ derived in Eq. (45), as being a search direction of the solution for the NAEs in Eq. (1).

### 3.6 The present algorithm driven by the best descent vector $\mathbf{u} = \alpha_c \mathbf{E} + \mathbf{D}^T \mathbf{E}$, without inverting D

Then, we can derive the following modified globally optimal iterative algorithm (MGOIA) to deal with the NAEs in Eq. (1):

(1) Choose $0 \le \gamma < 1$, and give an initial guess of $\mathbf{x}_0$.

(2) For $k$= 0, 1, 2… we repeat the following calculations:

$$\mathbf{q}_1^k = \mathbf{F}_k \mathbf{E}_k,$$

$$\mathbf{q}_2^k = \mathbf{D}_k \mathbf{E}_k,$$

$$a_c^k = \frac{\left\|\mathbf{q}_1^k\right\|^2 \left\|\mathbf{q}_2^k\right\|^2 - (\mathbf{q}_1^k \cdot \mathbf{q}_2^k)^2}{\left\|[\mathbf{q}_1^k, \mathbf{E}_k, \mathbf{q}_2^k]\right\|^2},$$

$$\alpha_c^k = \frac{a_c^k \mathbf{E}_k \cdot \mathbf{q}_1^k \mathbf{E}_k \cdot \mathbf{q}_2^k - \mathbf{q}_1^k \cdot \mathbf{q}_2^k}{\left\|\mathbf{q}_2^k\right\|^2 - a_c^k (\mathbf{E}_k \cdot \mathbf{q}_2^k)^2}, \quad (\text{critical } \alpha_c^k) \tag{58}$$

$$\mathbf{w}_k = \alpha_c^k \mathbf{E}_k + \mathbf{D}_k^T \mathbf{E}_k, \quad (\text{best descent vector})$$

$$\mathbf{q}_k = \mathbf{q}_1^k + \alpha_c^k \mathbf{q}_2^k,$$

$$\mathbf{x}_{k+1} = \mathbf{x}_k - (1-\gamma) \frac{\mathbf{E}_k^T \mathbf{q}_k}{\left\|\mathbf{q}_k\right\|^2} \mathbf{w}_k. \tag{59}$$

If $\mathbf{x}_{k+1}$ converges according to a given stopping criterion $\|\mathbf{E}_{k+1}\| < \varepsilon$, then stop; otherwise, go to step (2). In the above, we have excluded the common term $\|\mathbf{E}_k\|^2$ in Eqs. (55) and (56).

**Remark 2:** In the iterative process, it may occur that

$$\mathbf{E}_k \cdot \mathbf{q}_k = \mathbf{E}_k^T [\mathbf{D}_k \mathbf{D}_k^T + \alpha_c^k \mathbf{D}_k] \mathbf{E}_k = 0, \tag{60}$$

such that the above iterative scheme stagnates at a one point, i.e.,

$$\mathbf{x}_{k+1} = \mathbf{x}_k. \tag{61}$$

There are two situations which may cause the above condition; one is $\mathbf{E}_k = \mathbf{0}$ and another is that the matrix $\mathbf{D}_k \mathbf{D}_k^T + \alpha_c^k \mathbf{D}_k$ is singular at that point. In the first case of $\mathbf{E}_k = \mathbf{0}$ the solution is already obtained, and we do not need a special treatment of it. In the second case, we can set $\alpha_c^k = 0$ when $\mathbf{E}_k \cdot \mathbf{q}_k$ is very small, e.g. $\mathbf{E}_k \cdot \mathbf{q}_k \le 10^{-15}$, and re-run this step; such that we have

$$\mathbf{E}_k \cdot \mathbf{q}_k = \mathbf{E}_k^T \mathbf{D}_k \mathbf{D}_k^T \mathbf{E}_k = \left\|\mathbf{D}_k^T \mathbf{E}_k\right\|^2 > 0. \tag{62}$$

This special treatment of the singularity of the matrix $\mathbf{D}_k \mathbf{D}_k^T + \alpha_c^k \mathbf{D}_k$ can improve the stagnation of the iterative sequence of $\mathbf{x}_k$. Nevertheless, in all the computations below, we do not yet face this situation.

## 4 Nonlinear Poisson problems in heat diffusion and numerical examples

### 4.1 Example 1

In this example, we apply the proposed method to solve the following two-dimensional boundary value problem of nonlinear Poisson equation:

$$\Delta u = -(\frac{\partial u}{\partial y})^2 + 2y + x^4,\ 0 \le x \le 1, 0 \le y \le 1, \tag{63}$$

with the boundary conditions

$$\begin{aligned} &u(0,y) = 0,\ u(1,y) = y, \\ &u(x,0) = 0,\ u(x,1) = x^2. \end{aligned} \tag{64}$$

The exact solution is

$$u(x,y) = x^2 y. \tag{65}$$

By applying the new algorithm to solve the above equation in the domain of $0 \le x \le 1$ and $0 \le y \le 1$, we use $n_1 = n_2 = 5$, which are numbers of nodal points in a standard finite difference approximation of Eq. (57). The residual error and convergence rate are shown in Figs. 1(a) and 1(b), respectively. Under a convergence criterion $\varepsilon = 10^{-4}$, the present algorithm with $\gamma = 0.3$ can converge with 18 steps, and obtains an accurate solution with the maximum error $5.13 \times 10^{-7}$. The numerical solutions and errors are plotted in Figs. 2 and 3, respectively. Upon compared with the numerical results computed by Wang and Qin (2006) with the coupling virtual boundary collocation method with the radial basis functions and the analog equation method (see Table 2 of the above cited paper), we can find that the current scheme is much more accurate than the above-mentioned approach.

Table 1: Comparisons of Wang and Qin (2006), exact ones and errors.

| Location | Exact solutions | Errors of Wang and Qin (2006) | Errors of MGOIA |
|---|---|---|---|
| (0.00, 0.00) | 0.000000 | 0. | 0. |
| (0.25, 0.25) | 0.015625 | 2.8E-4 | 2.6E-7 |
| (0.50, 0.50) | 0.125000 | 1.0E-4 | 5.1E-7 |
| (0.75, 0.75) | 0.421875 | 3.0E-4 | 2.8E-7 |
| (1.00, 1.00) | 1.000000 | 0. | 0. |
| (1.00, 0.50) | 0.500000 | 0. | 0. |

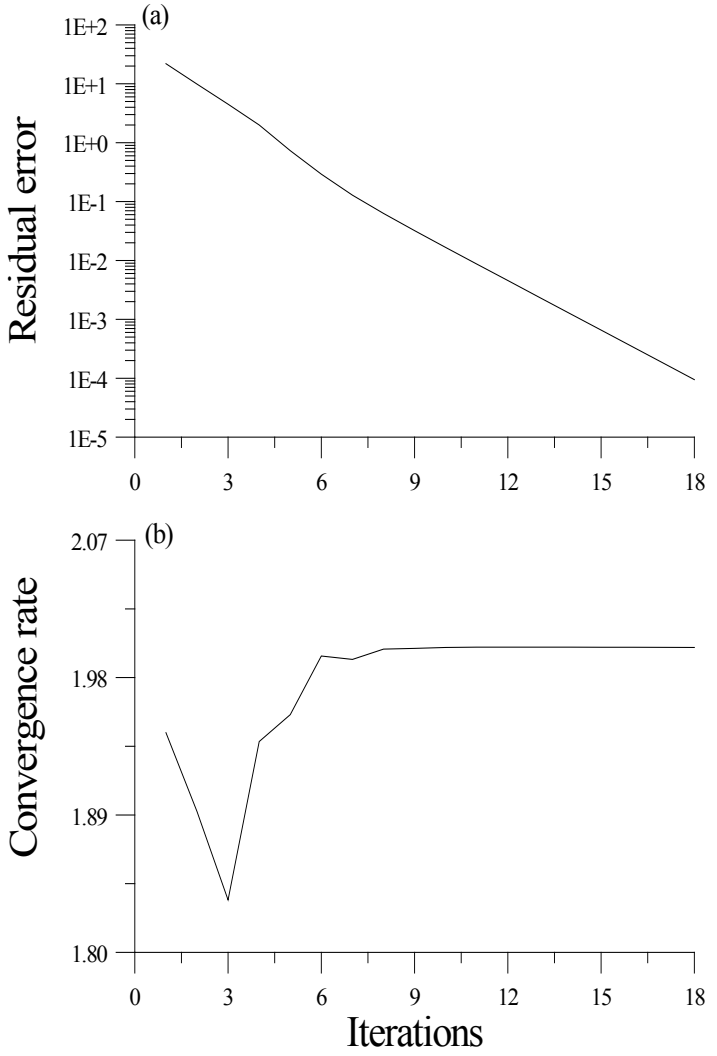


Figure 1: For example 1, solved by MGOIA, (a) the residual errors, and (b) the convergence rates.

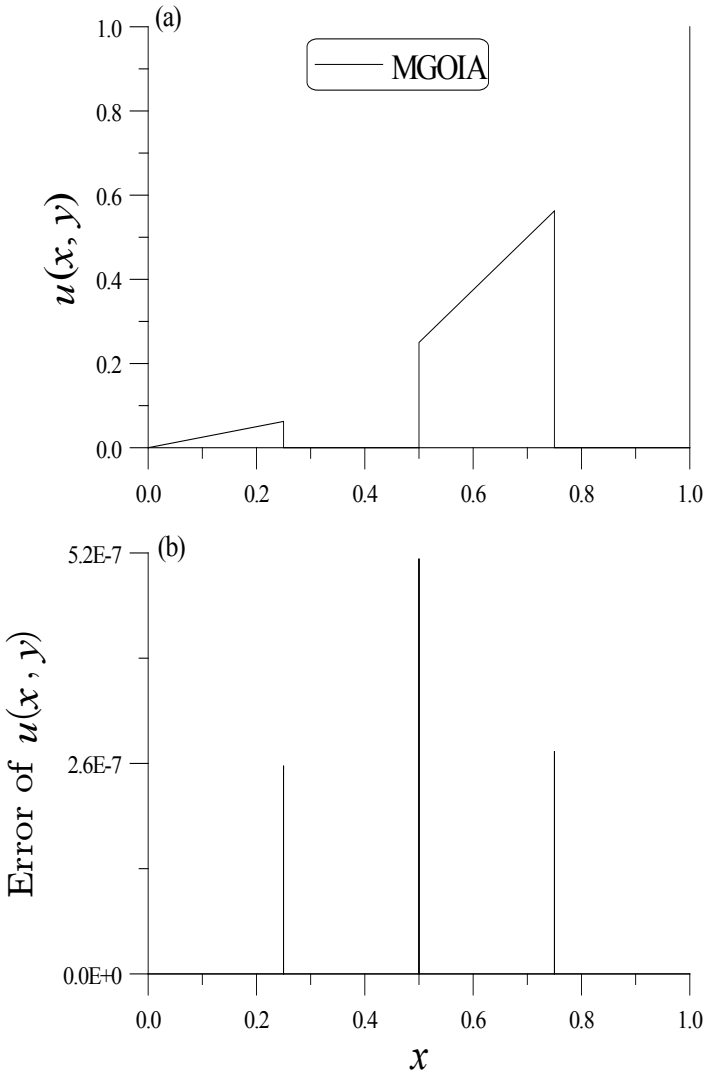


Figure 2: The results of MGOIA for Example 1 along the $x$-axis are plotted in (a) the numerical solutions, and (b) the numerical errors

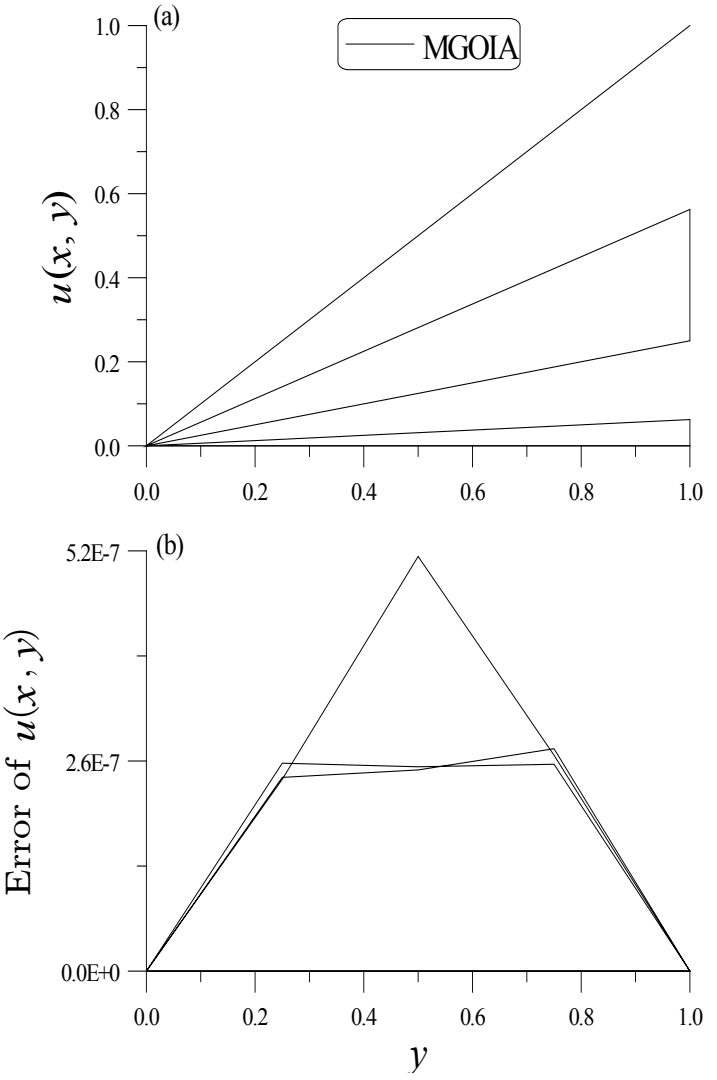


Figure 3: The results of MGOIA for Example 1 along the $y$-axis are plotted in (a) the numerical solutions, and (b) the numerical errors.

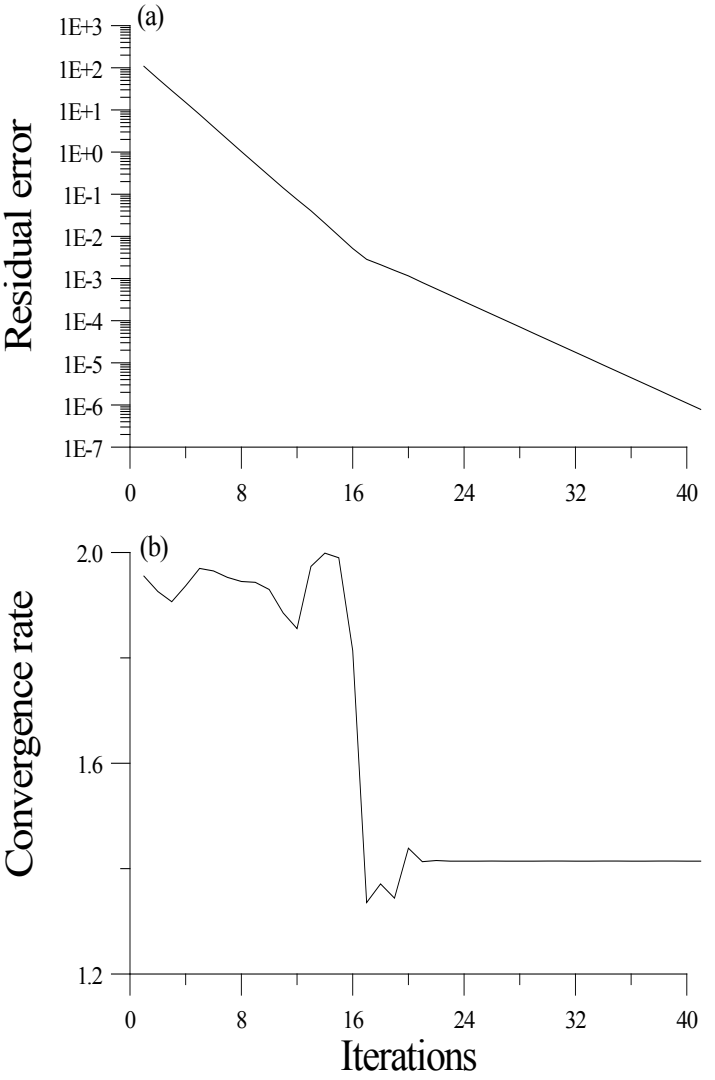


Figure 4: For example 2, solved by the MGOIA, (a) the residual errors, and (b) the convergence rate.

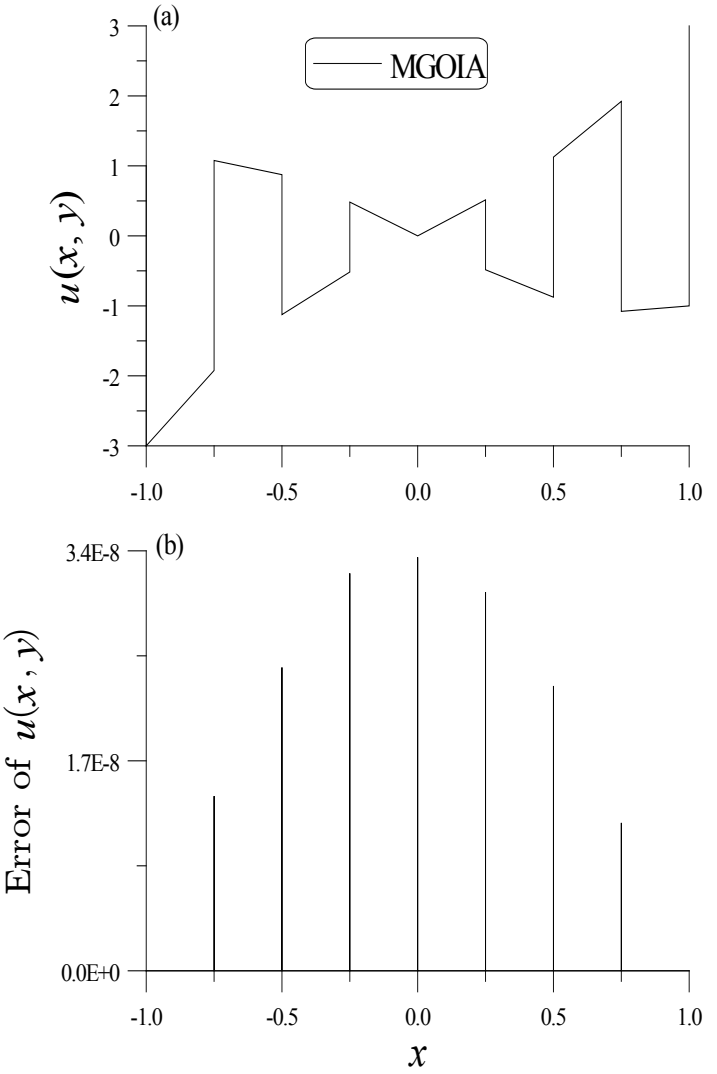


Figure 5: The results of MGOIA for Example 2 along the *x*axis are plotted in (a) the numerical solutions, and (b) the numerical errors.

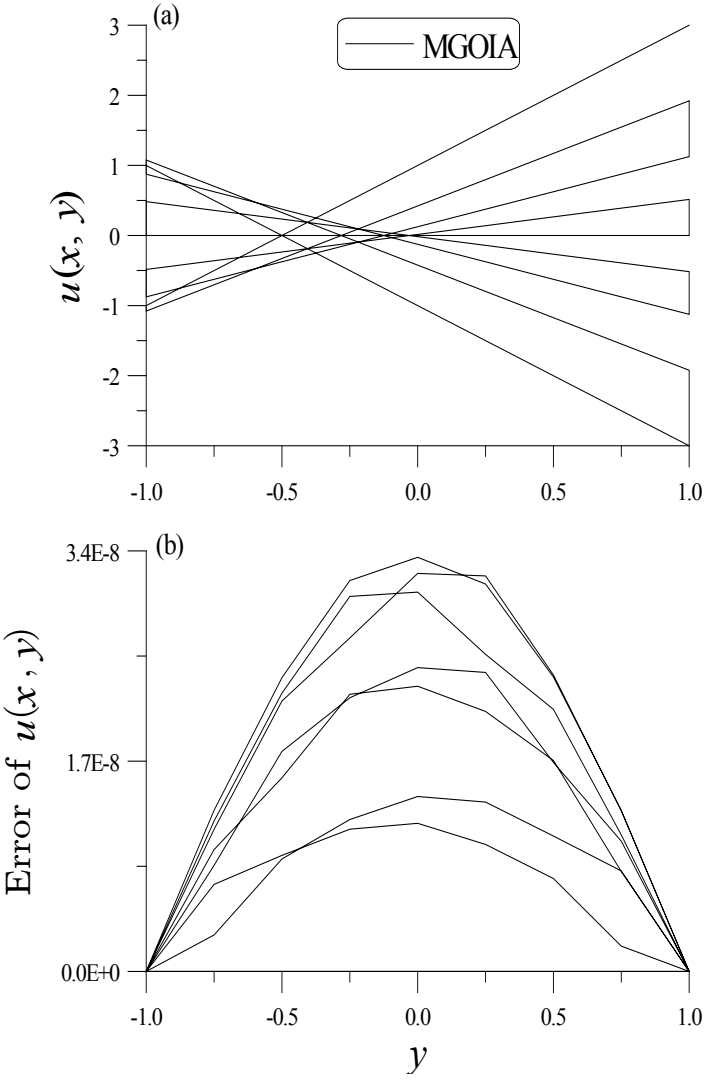


Figure 6: The results of MGOIA for Example 2 along the $y$-axis are plotted in (a) the numerical solutions, and (b) the numerical errors.

### 4.2 Example 2

Then, we ponder the following two-dimensional boundary value problem of nonlinear Poisson equation:

$$\Delta u = u^2 + 6x - x^6 - 4x^4 y - 4x^2 y^2, \ -1 \le x \le 1, \ -1 \le y \le 1, \tag{66}$$

with the boundary conditions

$$\begin{aligned} &u(-1,y) = -2y - 1, \ u(1,y) = 2y + 1, \\ &u(x,-1) = x^3 - 2x, \ u(x,1) = x^3 + 2x. \end{aligned} \tag{67}$$

The exact solution is

$$u(x,y) = x^3 + 2xy. \tag{68}$$

By using the proposed scheme to tackle the above equation in the domain of $-1 \le x \le 1$ and $-1 \le y \le 1$, we use $n_1 = n_2 = 9$, which are numbers of nodal points in a standard finite difference approximation of Eq. (66). The residual error and convergence rate are displayed in Figs. 4(a) and 4(b), respectively. Under a convergence criterion $\varepsilon = 10^{-6}$, the present approach with $\gamma = 0.1$ can converge with 41 steps, and attains an accurate solution with the maximum error $3.34 \times 10^{-8}$. The numerical solutions and errors are drawn in Figs. 5 and 6, respectively. Upon compared with the numerical results computed by Liu (2008) with the fictitious time integration method (FTIM) (see Fig. 2(b) of the above cited paper), the proposed algorithm is more accurate than the above-mentioned scheme.

### 4.3 Example 3

Let us further consider another two-dimensional boundary value problem of nonlinear elliptic equation:

$$\Delta u + \omega^2 u + \varepsilon u^3 = p(x,y), \ 0 \le x \le 1, 0 \le y \le 1, \tag{69}$$

with the boundary conditions

$$\begin{aligned} &u(0,y) = \tfrac{-5}{6} y^3, \quad u(1,y) = \tfrac{-5}{6}(y^3 + 1) + 3(y + y^2), \\ &u(x,0) = \tfrac{-5}{6} x^3, \quad u(x,1) = \tfrac{-5}{6}(x^3 + 1) + 3(x + x^2). \end{aligned} \tag{70}$$

The exact solution is

$$u(x,y) = \frac{-5}{6}(x^3 + y^3) + 3(x^2 y + x y^2). \tag{71}$$

By employing the present approach to resolve the above equation in the domain of $0 \le x \le 1$ and $0 \le y \le 1$, we use $n_1 = n_2 = 10$, which are numbers of nodal points in

a standard finite difference approximation of Eq. (69). The residual error and convergence rate are shown in Figs. 7(a) and 7(b), respectively. Under a convergence criterion $\varepsilon = 10^{-4}$, the present scheme with $\gamma = 0.1$ can converge with 41 steps, and acquires an accurate solution with the maximum error $7.35\times10^{-7}$. The numerical solutions and errors are depicted in Figs. 8 and 9, respectively. Upon compared with the numerical results in [Atluri and Zhu (1998a); Atluri and Zhu (1998b)] with that from the new meshless local Petrov-Galerkin approach, in [Zhu, Zhang and Atluri (1999)] with that from the local boundary integral equation method and the moving least squares approximation, in [Shen and Liu (2011)] with that from the new differential quadrature method and the FTIM (see Figs. 17-19 of the above cited paper), in [Liu, Dai and Atluri (2011a)] with that from the optimal iterative algorithms with optimal descent vectors (see Fig. 3 of the above cited paper), and in [Liu, Dai and Atluri (2011b)] with that from the different optimal iterative algorithms with optimal descent vectors (see Fig. 3 of the above cited paper), and in [Liu (2012)] with that from the manifold-based exponentially convergent algorithm (see Fig. 4 of the above cited paper), we can reveal that the MGOIA is more accurate than the above-mentioned schemes.

### *4.4 Example 4*

The following nonlinear diffusion reaction equation is contemplated:

$$\Delta u = 4u^3(x^2+y^2+a^2),\ -1 \le x \le 1,\ -1 \le y \le 1, \tag{72}$$

with the boundary conditions

$$\begin{aligned} u(-1,y) &= \tfrac{-1}{1+y^2-a^2},\ u(1,y) = \tfrac{-1}{1+y^2-a^2}, \\ u(x,-1) &= \tfrac{-1}{1+x^2-a^2},\ u(x,1) = \tfrac{-1}{1+x^2-a^2}. \end{aligned} \tag{73}$$

The exact solution is

$$u(x,y) = \frac{-1}{x^2+y^2-a^2} \tag{74}$$

is singular on the circle with a radius $a$.

For the square domain, Algahtani (2005) has solved this problem by using a radial basis method, whose results as shown there in Fig. 3 are not matched well to the exact solution. By employing the present approach to resolve the above equation in the domain of $-1 \le x \le 1$ and $-1 \le y \le 1$, we utilize $n_1 = n_2 = 17$, which are numbers of nodal points in a standard finite difference approximation of Eq. (72). At the point $y_0 = 0$ the error of $u$was plotted with respect to $x$in Fig. 10 by the dashed line, of which the maximum error is about $2.52\times10^{-4}$. At the point $x_0 = 05$

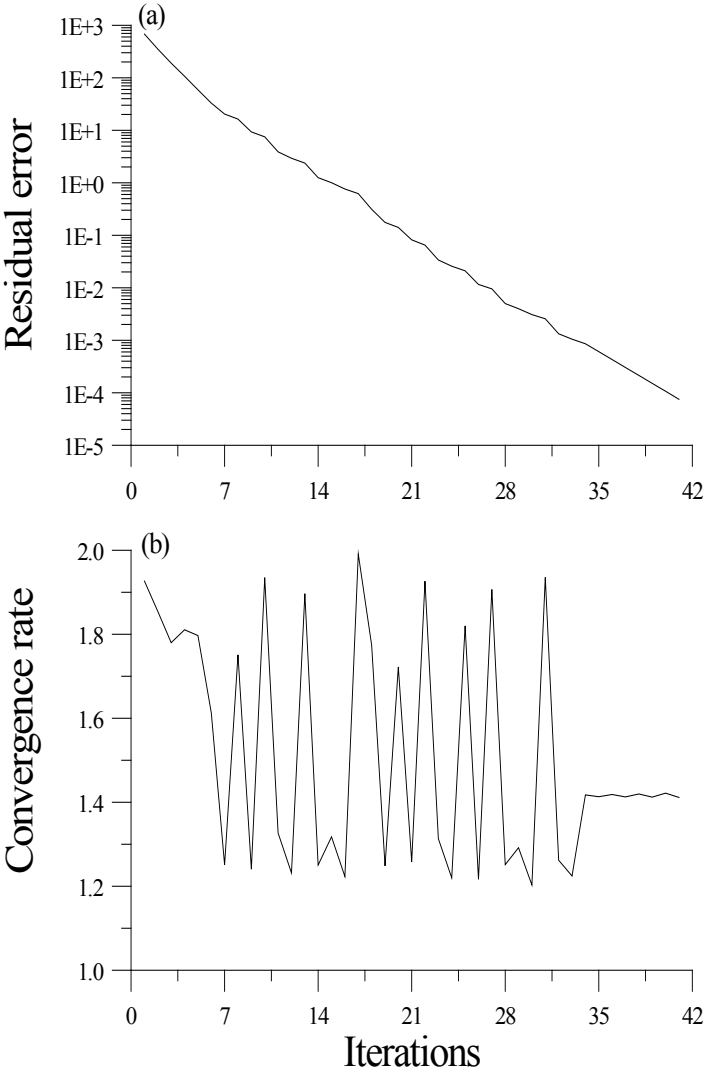


Figure 7: For example 3, solved by the MGOIA, (a) the residual errors, and (b) the convergence rate.

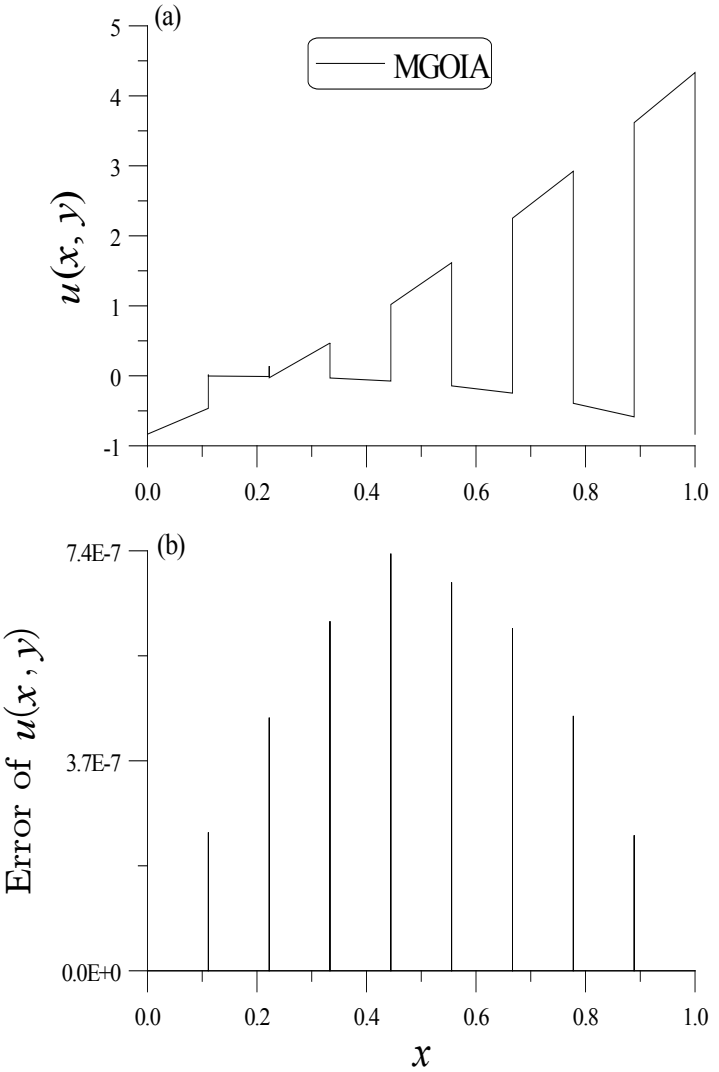


Figure 8: The results of MGOIA for Example 3 along the $x$-axis are plotted in (a) the numerical solutions, and (b) the numerical errors.

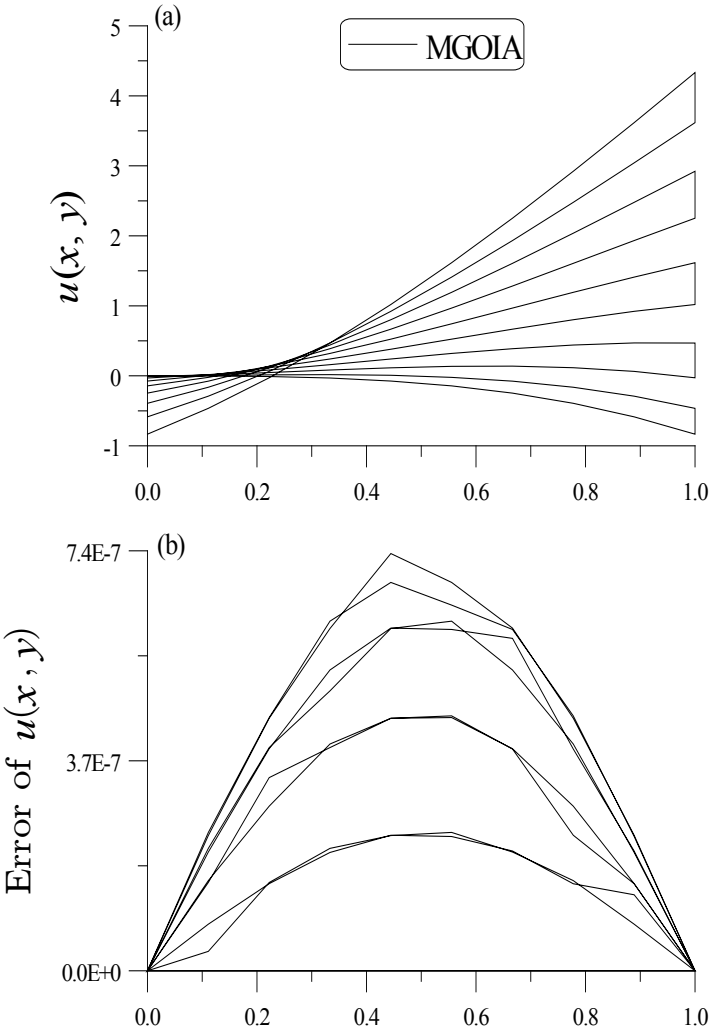


Figure 9: The results of MGOIA for Example 3 along the $y$-axis are plotted in (a) the numerical solutions, and (b) the numerical errors.

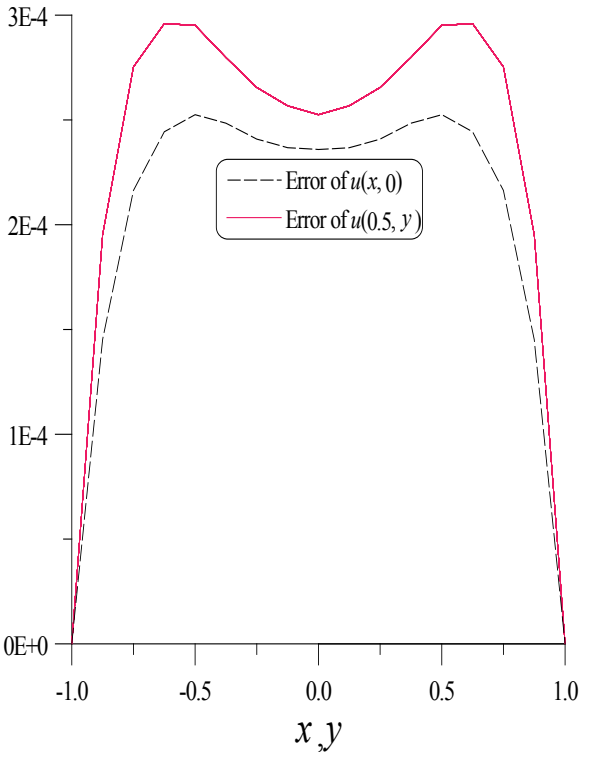


Figure 10: Plotting the numerical errors of Example 4 for $a$= 2 of a nonlinear reaction-diffusion equation in rectangular domain.

the error of $u$was plotted with respect to $y$in Fig. 10 by the solid line, of which the maximum error is about $3.05\times10^4$. Under a convergence criterion $\varepsilon = 10^{-2}$, the present algorithm with $\gamma = 0.1$ can converge with 45 steps. The numerical solutions and errors are illustrated in Figs. 11 and 12, respectively. Upon compared with the numerical results in Liu (2008) with the FTIM (see Fig. 3(a) of the above cited paper), the MGOIA is more accurate than the above-mentioned two approaches.

Besides, for the amoeba-like domain, one illustrious meshfree numerical approach to resolve the non-linear PDE of elliptic type is the radial basis function (RBF) scheme, which expands the solution $u$ by

$$u(x,y) = \sum_{k=1}^{n} a_k \phi_k, \tag{75}$$

where $a_k$ are the expansion coefficients to be determined and $\phi_k$ is a set of RBFs,

for instance,

$$\begin{aligned}
&\phi_k = (r_k^2 + c^2)^{N-3/2},\ N = 1,2,\ldots,\\
&\phi_k = r_k^{2N} \ln r_k,\ N = 1,2,\ldots,\\
&\phi_k = \exp\left(\tfrac{-r_k^2}{a^2}\right),\\
&\phi_k = (r_k^2 + c^2)^{N-3/2} \exp\left(\tfrac{-r_k^2}{a^2}\right),\ N = 1,2,\ldots,
\end{aligned} \tag{76}$$

where the radius function $r_k$ is given by $r_k = \sqrt{(x-x_k)^2 + (y-y_k)^2}$, in which $(x_k, y_k)$, $k = 1,\ldots, n$ are called source points. The constants $a$ and $c$ are shape parameters. In the below, we take the first set of $\phi_k$ as trial functions, which is known as a multi-quadric RBF [Golberg, Chen and Karur (1996); Cheng, Golberg, Kansa and Zammito (2003)], with $N = 2$. In this numerical experiment, we employ the multi-quadric radial basis function to solve Eq. (66), and $a = 4$ is fixed. The domain is an amoeba-like domain with

$$\rho(\theta) = (\sin 2\theta)^2 \exp(\sin\theta) + (\cos 2\theta)^2 \exp(\cos\theta). \tag{77}$$

Inserting Eq. (75) into Eq. (72) and placing some field points inside the domain to satisfy the governing equation and some points on the boundary to gratify the boundary condition, we can derive $n$ NAEs to select the $n$ coefficients $a_k$. The source points $(x_k, y_k)$, $k = 1, \ldots, n$ are uniformly distributed on a contour given by $R_0 + \rho(\theta)$, in which $\theta_k = 2k\pi/n$. The residual error and convergence rate are shown in Figs. 13(a) and 13(b), respectively. Under a convergence criterion $\varepsilon = 0.01$, $R_0$= 0.4, and $c = 0.5$, the current method with $\gamma = 0.13$ can converge with 288 steps, and acquires an accurate solution with the maximum error $2.68\times10^{-3}$. The numerical solutions and errors are exhibited in Figs. 14 and 15, respectively.

Upon compared with the numerical results in Liu (2009) with the FTIM (see Fig. 7 of the above cited paper), ,in [Liu and Atluri (2011)] with that from the optimal vector driven algorithm (see Fig. 16 of the above cited paper), in [Liu, Dai and Atluri (2011a)] with that from the optimal iterative algorithms with optimal descent vectors (see Fig. 2 of the above cited paper), and in [Liu, Dai and Atluri (2011b)] with that from the different optimal iterative algorithms with optimal descent vectors (see Fig. 2 of the above cited paper), and in [Liu (2012)] with that from the manifold-based exponentially convergent algorithm (see Fig. 2 of the above cited paper), we can show that the MGOIA is more accurate than the above-mentioned schemes.

## 5 Conclusions

In this paper, we have derived the switch criterion to accelerate the convergence speed of globally optimal iterative algorithm (GOIA), which was called modified

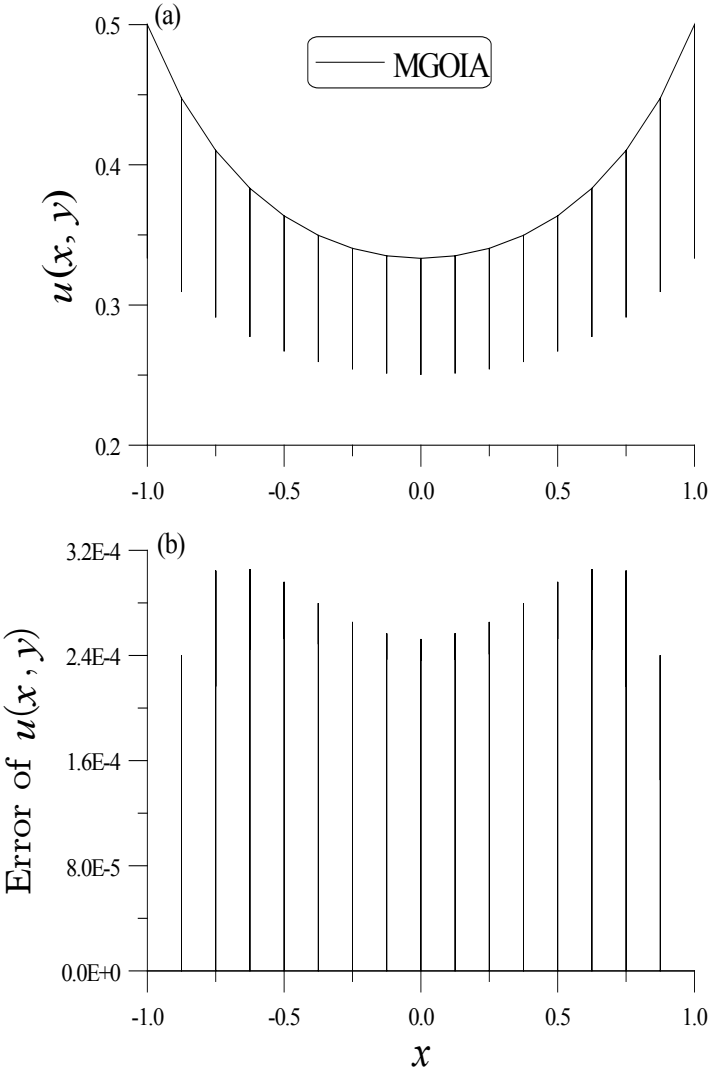


Figure 11: The results of MGOIA for Example 4 in rectangular domain along the $x$-axis are plotted in (a) the numerical solutions, and (b) the numerical errors.

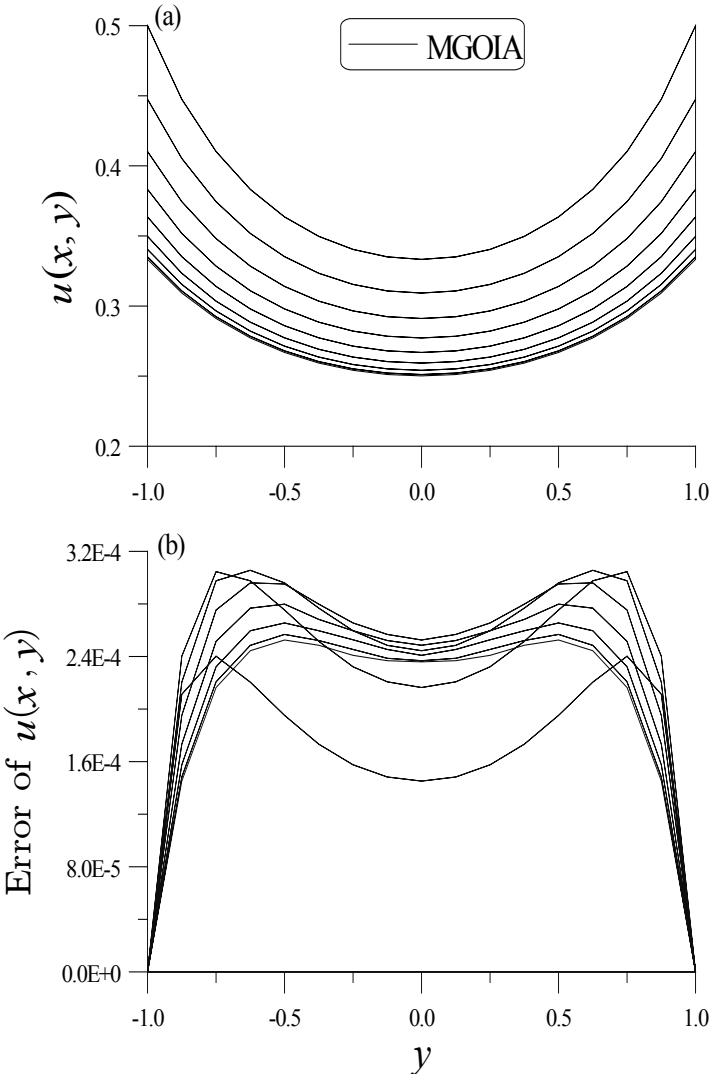


Figure 12: The results of MGOIA for Example 4 in rectangular domain along the $y$-axis are plotted in (a) the numerical solutions, and (b) the numerical errors.

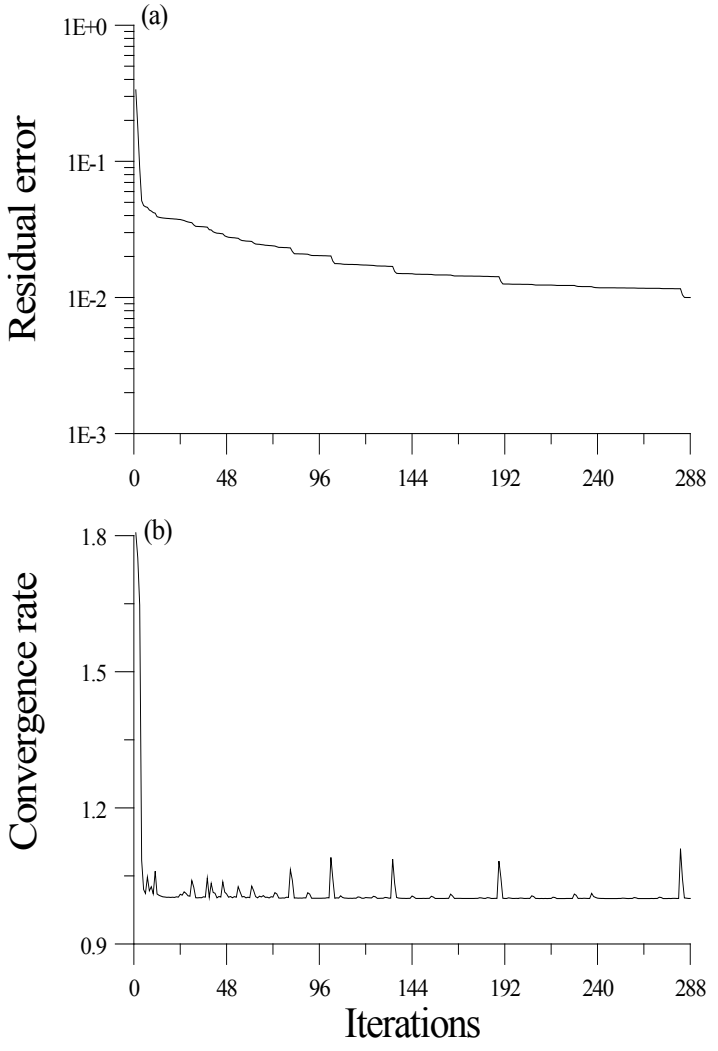


Figure 13: For example 4 in amoeba-like domain, solved by the MGOIA, (a) the residual errors, and (b) the convergence rate.

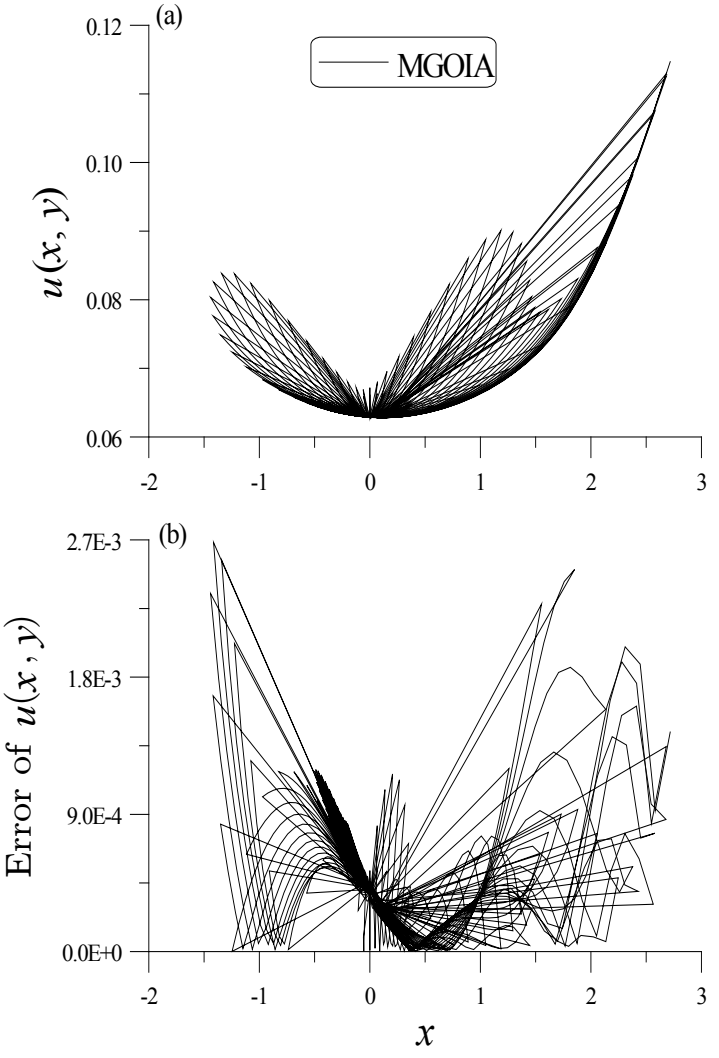


Figure 14: The results of MGOIA for Example 4 in amoeba-like domain along the $x$-axis are plotted in (a) the numerical solutions, and (b) the numerical errors.

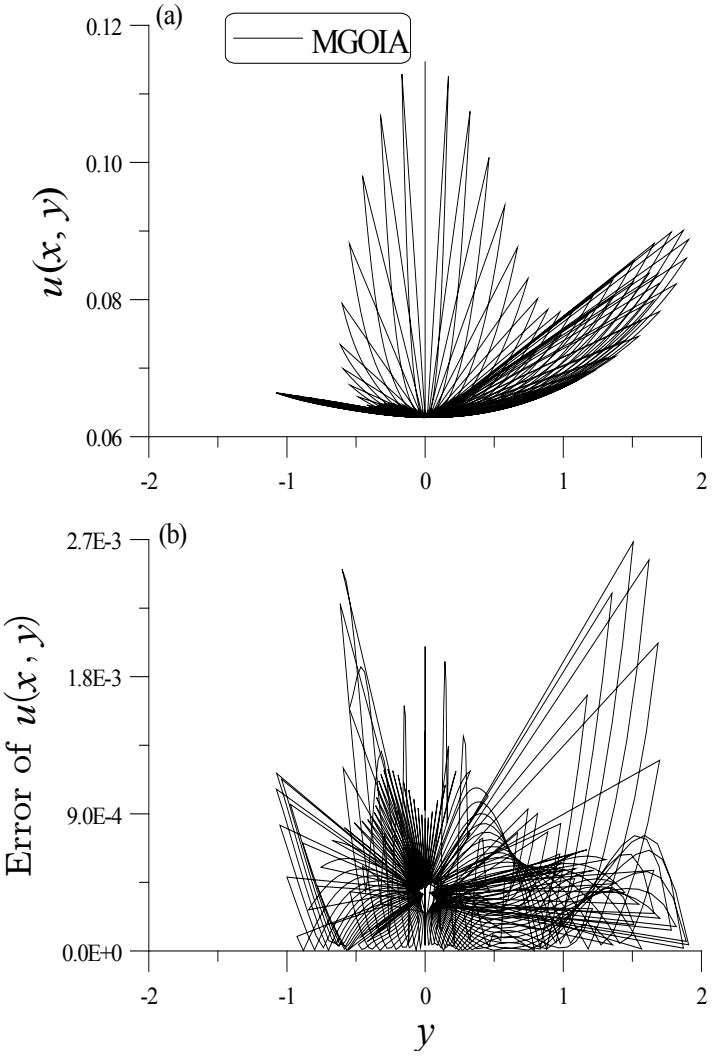


Figure 15: The results of MGOIA for Example 4 in amoeba-like domain along the $y$-axis are plotted in (a) the numerical solutions, and (b) the numerical errors.

globally optimal iterative algorithm (MGOIA). The proposed approach is convergent automatically, and without calculating the inversions of the Jacobian matrices. It can solve a large system of nonlinear algebraic equations with a few iterations. On the basis of those numerical experiments, we exhibit that the MGOIA is applicable to the nonlinear Poisson problems in heat diffusion and validate the accuracy and efficiency of the proposed approach. The numerical errors of our scheme are in the order of $O(10^{-3})$–$O(10^{-8})$.

## References

**Algahtani, H. J.** (2006): A meshless method for non-linear Poisson problems with high gradients. *Comput. Assist. Mech. Eng. Sci.*, vol. 13, pp. 367-377.

**Atluri, S. N.; Zhu, T. L.** (1998a): A new meshless local Petrov-Galerkin (MLPG) approach in computational mechanics. *Comput. Mech.*, vol. 22, pp. 117-127.

**Atluri, S. N.; Zhu, T. L.** (1998b): A new meshless local Petrov-Galerkin (MLPG) approach to nonlinear problems in computer modeling and simulation. *Comput. Model Simul Eng*, vol. 3, pp. 187-196.

**Balakrishnan, K.; Ramachandran, P. A.** (1999): A particular solution Trefftz method for non-linear Poisson problems in heat and mass transfer. *J. Comput. Phys.*, vol. 150, pp. 239-267

**Balakrishnan, K.; Ramachandran, P. A.** (2001): Osculatory interpolation in the method of fundamental solution for nonlinear Poisson problems. *J. Comput. Phys.*, vol. 172, pp. 1-18

**Cheng, A. H. D.; Golberg, M. A.; Kansa, E. J.; Zammito, G.** (2003): Exponential convergence and *Hc* multiquadric collocation method for partial differential equations. *Numer. Meth. Part. Diff. Eqs.*, vol. 19, pp. 571-594.

**Golberg, M. A.** (1995): The method of fundamental solutions for Poisson's equation. *Eng. Anal. Bound. Elem.*, vol. 16, pp. 205-213.

**Golberg, M. A.; Chen, C. S.; Karur, S. R.** (1996): Improved multiquadric approximation for partial differential equations. *Eng. Anal. Bound. Elem.*, vol. 18, pp. 9-17.

**Gu, G. G.** (1991): Boundary element methods for solving Poisson equations in computer vision problems. *Computer Vision and Pattern Recognition. Proceedings CVPR '91., IEEE Computer Society Conference on*, pp. 546-551.

**Kasab, J. J.; Karur, S. R.; Ramachandran, P. A.** (2001): Quasilinear boundary element method for nonlinear Poisson type problems. *Eng. Anal. Bound. Elem.*, vol. 15, pp. 277-282.

**Liu C-S.** (2008): A fictitious time integration method for two-dimensional quasilin-

ear elliptic boundary value problems. *CMES: Computer Modeling in Engineering & Sciences*, vol. 33, pp. 179-198.

**Liu, C.S.** (2009): A fictitious time integration method for a quasilinear elliptic boundary value problem, defined in an arbitrary plane domain. *CMC: Computers, Materials & Continua* vol. 11, pp. 15–32

**Liu, C.-S.** (2012): A manifold-based exponentially convergent algorithm for solving non-linear partial differential equations. *J. Mar. Sci. Tech.*, vol. 20, pp. 441-449.

**Liu, C.-S.; Atluri, S. N.** (2012): A globally optimal iterative algorithm using the best descent vector $\dot{\mathbf{x}} = \lambda[\alpha_c \mathbf{F} + \mathbf{B}^T\mathbf{F}]$, with the critical value $\alpha_c$, for solving a system of nonlinear algebraic equations $\mathbf{F}(\mathbf{x}) = \mathbf{0}$. *CMES: Computer Modeling in Engineering & Sciences*, vol. 84, pp. 575-601.

**Liu, C.-S.; Dai, H. H.; Atluri, S. N.** (2011a): A further study on using $\dot{\mathbf{x}} = \lambda[\alpha\mathbf{R} + \beta\mathbf{P}]$ $(\mathbf{P} = \mathbf{F} - \mathbf{R}(\mathbf{F}\cdot\mathbf{R})/\|\mathbf{R}\|^2)$ and $\dot{\mathbf{x}} = \lambda[\alpha\mathbf{F} + \beta\mathbf{P}^*](\mathbf{P}^* = \mathbf{R} - \mathbf{F}(\mathbf{F}\cdot\mathbf{R})/\|\mathbf{F}\|^2)$in iteratively solving the nonlinear system of algebraic equations $\mathbf{F}(\mathbf{x}) = \mathbf{0}$. *CMES: Computer Modeling in Engineering & Sciences*, vol. 81, pp. 195-227.

**Liu, C.-S.; Dai, H. H.; Atluri, S. N.** (2011b): Iterative solution of a system of nonlinear algebraic equations $\mathbf{F}(\mathbf{x}) = \mathbf{0}$, using $\dot{\mathbf{x}} = \lambda[\alpha\mathbf{R} + \beta\mathbf{P}]$ or $\dot{\mathbf{x}} = \lambda[\alpha\mathbf{F} + \beta\mathbf{P}^*]$, $\mathbf{R}$ is a normal to a hyper-surface function of $\mathbf{F}$, $\mathbf{P}$ normal to $\mathbf{R}$, and $\mathbf{P}^*$ normal to $\mathbf{F}$. *CMES: Computer Modeling in Engineering & Sciences*, vol. 81, pp. 335-362.

**Shen, Y. H.; Liu C-S.** (2011): A new insight into the differential quadrature method in solving 2-D elliptic PDEs. *CMES: Computer Modeling in Engineering & Sciences* vol. 71, pp. 157-178.

**Tri, A.; Zahrouni, H.; Potier-Ferry, M.** (2011): Perturbation technique and method of fundamental solution to solve nonlinear Poisson problems. *Eng. Anal. Bound. Elem.*, vol. 35, pp. 273-278.

**Tri, A.; Zahrouni, H.; Potier-Ferry, M.** (2012): High order continuation algorithm and meshless procedures to solve nonlinear Poisson problems. *Eng. Anal. Bound. Elem.*, vol. 36, pp. 1705-1714.

**Wang, H.; Qin, Q. H.** (2006): A meshless method for generalized linear or nonlinear Poisson-type problems. *Eng. Anal. Bound. Elem.*, vol. 30, pp. 515-521

**Wang, H.; Qin, Q. H.; Liang, X. P.** (2012): Solving the nonlinear Poisson-type problems with F-Trefftz hybrid finite element model. *Eng. Anal. Bound. Elem.*, vol. 36, pp. 39-46

**Whiteman, J. R.** (1974): Lagrangian finite element and finite difference methods for Poisson problems. *Maths Technical Papers (Brunel University)*, pp. 1-24.

**Zhu, T.; Zhang, J.; Atluri, S. N.** (1999): A meshless numerical method based on

the local boundary integral equation (LBIE) to solve linear and non-linear boundary value problems. *Eng. Anal. Bound. Elem.*, vol. 23, pp. 375-389